Available online at www.sciencedirect.com
SCIENCE DIRECT®
Journal of Chromatography A, 989 (2003) 95–108
JOURNAL OF CHROMATOGRAPHY A
www.elsevier.com/locate/chroma

Multiobjective optimization of simulated moving bed and Varicol processes using a genetic algorithm

Ziyang Zhang[a], Marco Mazzotti[b], Massimo Morbidelli[a,*]

[a]*Swiss Federal Institute of Technology Zurich, Laboratorium für Technische Chemie/LTC, ETH-Hönggerberg/HCI, CH-8093 Zürich, Switzerland*

[b]*ETH Zürich, Institut für Verfahrenstechnik, Sonneggstrasse 3, CH-8092 Zürich, Switzerland*

Abstract

The size of the packing material, the total number of columns and the total feed concentration have significant impacts on the economics of a preparative chromatographic separation, through their effects on column pressure drop, column efficiency and thermodynamics. In this work, the role of these parameters on the performances of a simulated moving bed and a Varicol process is investigated on a chiral separation system from literature, using an equilibrium stage model. A multiple objective optimization technique based on a genetic algorithm is adopted, which allows to maximize simultaneously the purity of the extract and productivity of the unit. In this way, it is possible to optimize and compare the performances of both processes in a wide range of parameter values, so as to assess their relative potential under equally optimized conditions. The optimization results, i.e. the so-called Pareto sets, have been discussed in the frame of equilibrium theory and the roles of these three parameters have been clarified.

Keywords: Optimization; Preparative chromatography; Mathematical modelling; Simulated moving bed chromatography; Varicol process

1. Introduction

Simulated moving bed (SMB) is a well established technology for performing continuous chromatographic separations covering all scales of possible interest in applications. In particular, it is now a crucial technology for optical enantiomer separations, which are currently under strong demand for industrial applications, mainly due to the more stringent drug administration policies. The design and optimization of these units can be done in the frame of equilibrium theory, i.e. neglecting transport limitation, using the so-called triangle theory [1–5] or using more detailed simulation models in connection with various optimization strategies [6–14].

The SMB unit has been originally devised as a practical realization of a true moving bed (TMB) unit where the two phases move countercurrently. A schematic diagram of a typical four-section SMB is shown in Fig. 1. The counter-current movement of the solid and the fluid is simulated by moving periodically the feed and withdrawal ports by one column in the direction of the fluid flow, with a predetermined period or switching time, t_s. Switching time and column configuration (the number of columns in each section) remain constant during the entire operation in order to simulate the constant solid flow-rate in a TMB. In contrast to SMB, the

*Corresponding author. Tel.: +41-1-632-3034; fax: +41-1-632-1082.
E-mail address: morbidelli@tech.chem.ethz.ch (M. Morbidelli).

0021-9673/02/$ – see front matter
PII: S0021-9673(02)01802-2

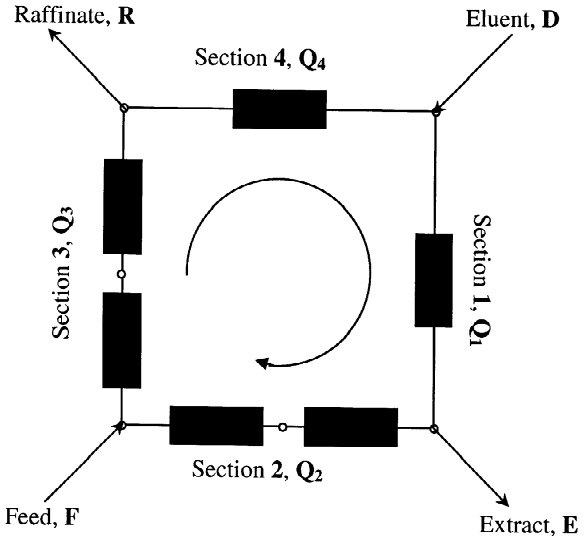

Fig. 1. Schematic diagram of a six-column SMB unit.

Varicol process, first reported by Ludemann-Hombourger et al. [15], is based on non-simultaneous and unequal shifts of the inlet and outlet ports. The operation diagrams of a SMB and a four-subinterval Varicol are compared in Fig. 2 for a six-column set-up. Within one (global) switching period t_s, the column configuration of Varicol changes from 1/2/2/1 (first subinterval) to 2/1/2/1 (second subinterval) by shifting the extract port by one column forward, then to 2/2/1/1 (third subinterval) by shifting the feed port one column forward, then to 1/2/1/2 (last subinterval) by shifting the eluent port one column forward, and finally returns back to the original configuration 1/2/2/1 by shifting the raffinate port one column forward. It is evident that compared to the SMB, in the Varicol the number of columns in each section changes during one switching period, so that the time-averaged number of columns in each section is not necessarily an integer (i.e. 1.5/1.75/1.5/1.25 in the example above). Accordingly, the Varicol process has more degrees of freedom than the corresponding SMB, which can be identified in a better tunable distribution of the columns in the sections of the unit.

Using two practical examples (the chiral separations of the 1,2,3,4-tetrahydro-1-naphthol racemate and of the SB-553261 racemate), Ludemann-Hombourger et al. [15,16] have shown experimentally

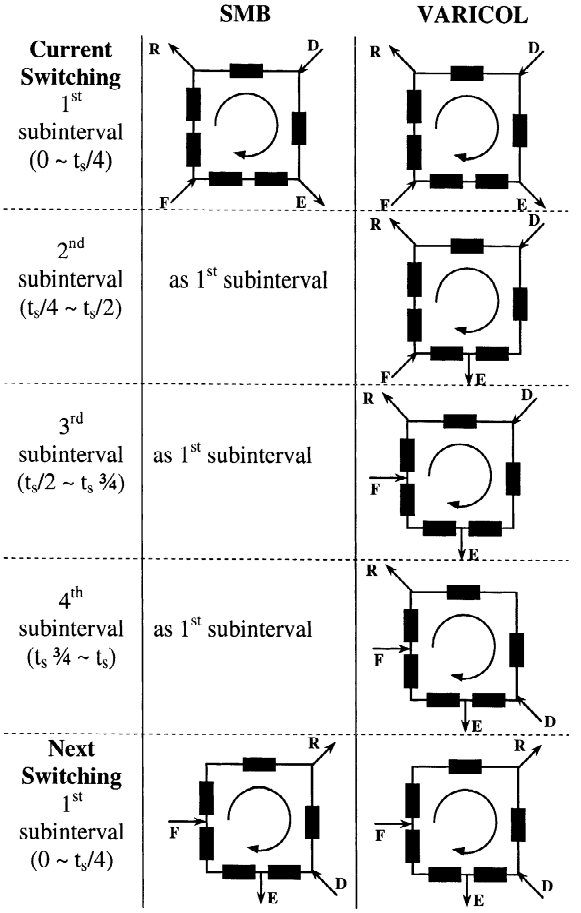

Fig. 2. Operation diagrams of SMB and four-subinterval Varicol units: scheduling of the port switching.

that Varicol achieves better performances than SMB, in terms of both increased specific productivity and reduced eluent consumption. In an earlier work [14], a systematic multiobjective optimization study of SMB and Varicol processes was presented, using an optimization technique based on the non-dominated sorting genetic algorithm [17]. Since in each case we have two conflicting objectives, the solution of the optimization problem is given by an optimum Pareto set, which is a set of operating conditions such that when moving from one to another, one of the objectives improves but the other worsens, and no operating condition can be found that would lead to objective values which are both better than those in the Pareto set. For both problems the optimal Pareto

Table 1
Characteristics of the model chiral separation system [11]

External porosity	$\varepsilon_b = 0.565$
Internal porosity	$\varepsilon_p = 0$
Isotherms	$\overline{C_A} = \frac{1.25C_A}{1 + 0.125C_A + 0.1C_B}$
	$\overline{C_B} = \frac{1C_B}{1 + 0.125C_A + 0.1C_B}$
Column configuration	$V_{solid} = 120$ ml; section $\Omega = 1$ cm^2
Maximum unit pressure drop	$(\Delta P_{unit})_{max} = 70$ bar
Van Deemter equation	HETP (cm) $= 0.0005 d_p$ (μm) $+ 0.00165 d_p^2 u$ (cm/s) $+ 0.001/u$
Pressure drop correlation	ΔP (bar) $= 960 u / d_p^2 L_{col}$ (cm)

sets have been computed for SMB and Varicol units, and confirmed that Varicol is superior to SMB in terms of treating more feed using less eluent or producing better quality products for fixed productivity and solvent consumption.

The developed optimization procedure allows to compare in a wide range of operating conditions the two processes, each optimized with respect to the same pair of objectives. This is a rare situation which allows to investigate and compare the full potential of SMB and Varicol. In this work we address this point by focusing on three variables which have a large impact on the economy of a chromatographic separation, particularly at large scale: the particle size of the packing material, the total number of columns and the feed concentration. As a model system we consider the chiral separation reported by Biressi et al. [11], whose relevant characteristics are summarized in Table 1, and examine the case where we want to maximize simultaneously the purity of the extract and the productivity of the unit, while the eluent consumption is unconstrained and the purity of the raffinate and the unit pressure drop are lower and upper bounded, respectively.

2. Background to the optimization problem

The design of SMB separations has been discussed extensively in the literature [2–5,10,18]. A synthetic picture of all possible performances of a SMB unit can be obtained, in the frame of equilibrium theory, through the so-called triangle theory. This is based on four dimensionless parameters, i.e. the flow-rate ratios, m_j, in the four sections of the unit (see Section 7 for the meaning of the symbols):

$$m_j = \frac{Q_j t_s - V_{col}\varepsilon}{V_{col}(1-\varepsilon)} \quad (j = 1, \ldots, 4) \tag{1}$$

Once the lower bound on m_1 and the upper bound on m_4 are satisfied, the operating conditions leading to complete separation form in the $(m_2 - m_3)$ parameter plane a region with triangular shape, where the vertex corresponds to the optimal condition in the sense that productivity is maximized while eluent consumption is minimized. This region depends only on the adsorption isotherm of the components to be separated and on the feed concentration. For the particular separation considered in this work, it has been calculated according to Gentilini et al. [19] and is shown in Fig. 3 for four different feed concentration values. It is seen that as the feed concentration increases, the complete separation region becomes smaller and sharper, while the optimal operating point moves downwards to the left in the $(m_2 - m_3)$ plane.

In addition to flow-rate ratios, adsorption isotherm and feed concentration, the operation and design of SMB also depend on the configuration of the set-up, including total number and dimension of columns, distribution of columns in each section and properties of the packing materials, as well as various practical constraints such as pressure drop and product purity (or yield). Of particular interest in large-scale applications is the selection of the particle size. For a given packing material, in fact the particle size significantly affects the SMB performance

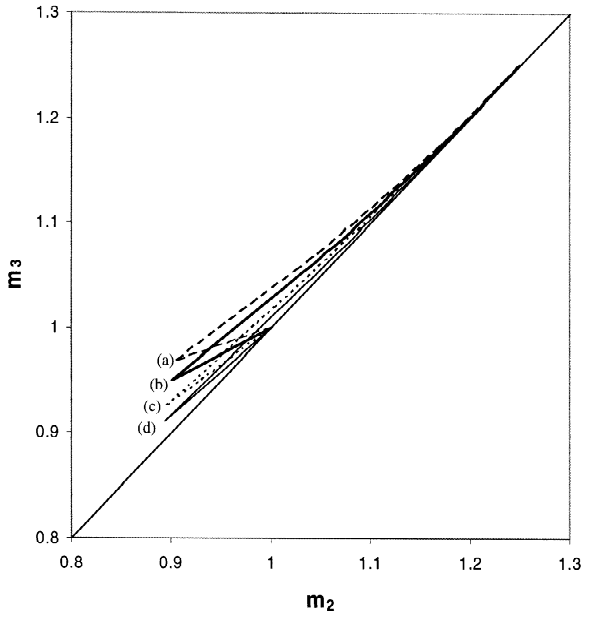

Fig. 3. Complete separation region in the (m_2, m_3) plane for the binary separation described in Table 1. (a) $C_T^F=6$ g/l; (b) $C_T^F=8$ g/l; (c) $C_T^F=14$ g/l; (d) $C_T^F=24$ g/l.

through column pressure drop and column efficiency. The former is given in the laminar flow regime by the Blake–Kozeny equation:

$$\frac{\Delta P_j}{L_{col}} = \frac{(1-\varepsilon_b)^2}{\varepsilon_b^3} \cdot \frac{150\mu}{d_P^2} \cdot u_j = \frac{\varphi}{d_P^2} \cdot u_j \quad (2)$$

where ΔP_j is the pressure drop per column in the jth section of the SMB, L_{col} the column length, u_j the superficial velocity in the jth section, ε_b the bed porosity, μ the fluid viscosity, and d_p the particle diameter. The column efficiency is expressed by the HETP, which is given as a function of particle diameter and fluid velocity by:

$$\mathrm{HETP}_j = ad_P + bd_P^2 u_j + c/u_j \quad (3)$$

where the first term representing eddy diffusivity depends linearly on the particle diameter, while the second indicating the effect of intraparticle mass transfer resistance exhibits a second-order dependence on the particle diameter, and the last represents molecular diffusion and is not related to particle size. The values of the parameters φ, a, b and c for the separation under examination are reported in Table 1 [11].

From the above equations, it is readily seen that larger particles, on the one hand, imply lower pressure drop and then allow for higher flow-rate and productivity, while on the other hand, lead to lower column efficiency, thus to poorer performance. This means that the particle size has conflicting effects on productivity and product purity, and therefore requires multiple objective optimization to be selected properly.

3. Modeling of SMB and Varicol

Various models have been applied to the modeling of chromatographic processes [20]. The equilibrium stage model is probably the best compromise between accuracy and computation time for high-performance preparative chromatography, and therefore it appears well suited for genetic algorithm (GA) optimization, which usually requires thousands of simulations per optimization problem. In this model, each column is modeled as a series of well mixed cells, in each of which equilibrium conditions are reached between the solid phase and the mobile phase. For a SMB unit during the Nth switching period, the mass balance equation for the ith component in the kth mixing cell is given by:

$$C_{i,N}^{(k-1)} = C_{i,N}^{(k)} + \left[\frac{t_0(j)}{N_{NTP}}\right] \cdot \frac{dC_{i,N}^{(k)}}{dt} + \left[\frac{1-\varepsilon}{\varepsilon}\right] \cdot \left[\frac{t_0(j)}{N_{NTP}}\right] \cdot \frac{\overline{dC_{i,N}^{(k)}}}{dt} \quad 0 \le t \le t_s \quad (4)$$

For a three-subinterval Varicol process during the Mth sub-interval of the Nth switching period, the corresponding mass balance is given by:

$$C_{i,N,M}^{(k-1)} = C_{i,N,M}^{(k)} + \left[\frac{t_0(j)}{N_{NTP}}\right] \cdot \frac{dC_{i,N,M}^{(k)}}{dt} + \left[\frac{1-\varepsilon}{\varepsilon}\right] \cdot \left[\frac{t_0(j)}{N_{NTP}}\right] \cdot \frac{\overline{dC_{i,N,M}^{(k)}}}{dt} \quad 0 \le t \le t_s/3; \quad M = 1, 2 \text{ or } 3 \quad (5)$$

In these equations $t_0(j)$ is the residence time of a

nonadsorbed species in a column in section j and is given by:

$$t_0(j) = \frac{\varepsilon V_{\text{col}}}{Q_j} \tag{6}$$

where Q_j is the volumetric flow-rate in section j, and ε is the column porosity. N_{NTP} is the number of theoretical stages in each column, which is averaged over all sections in the SMB as follows:

$$N_{\text{NTP}} = \frac{\sum_{j=1}^{4}\left(\frac{L_{\text{col}} \cdot n_j}{\text{HETP}_j}\right)}{N_{\text{col}}} \tag{7}$$

where N_{col} and n_j indicate the number of columns in the entire unit and in section j, respectively. In the case of Varicol, N_{NTP} is further averaged over all column configurations.

An important aspect in the performed simulations is the criteria adopted to establish when steady state conditions are reached. Two criteria have been used in the following. The first is based on the mass balance closure. The following quantity is computed after each switching period of index N:

$$E_N = \left[1 - \frac{M^{\text{R}}_{A,N} + M^{\text{E}}_{A,N}}{M^{\text{F}}_{A,N}}\right]^2 + \left[1 - \frac{M^{\text{R}}_{B,N} + M^{\text{E}}_{B,N}}{M^{\text{F}}_{B,N}}\right]^2 \tag{8}$$

where $M^{\text{R}}_{i,N}$, $M^{\text{E}}_{i,N}$ and $M^{\text{F}}_{i,N}$ are the masses of component i collected in the raffinate and extract, and introduced into the feed during the Nth switching period, respectively. This criterion is satisfied when the calculated error is $E_N < 4\times10^{-4}$. In addition, we require that the computed solution remains unchanged over a switching period, i.e. steady state conditions are achieved, by enforcing that:

$$|E_N - E_{N-1}| < 1\times10^{-8} \tag{9}$$

Finally, note that Eqs. (4) and (5) with the associate set of initial and boundary conditions [14] are solved using the subroutine DIVPAG (based on Gear's method) of the IMSL library.

4. Multiobjective optimization procedures

Depending upon the particular separation problem under examination, the objective functions of primary interest may be different. In the following, we consider a typical multiobjective optimization problem relevant in applications, where we want to simultaneously maximize the purity of the extract and the productivity. In addition, a minimum 90% purity of the raffinate product is required as well as a maximum 70 bar pressure drop along the entire unit, i.e. $\Delta P_{\text{unit}} \leq 70$ bar, where:

$$\Delta P_{\text{unit}} = \sum_{j=1}^{4} n_j \Delta P_j \tag{10}$$

In the case of the Varicol process, the value of ΔP_{unit} is taken as the highest among those computed in each subinterval. The considered optimization problem is represented mathematically as follows:

$$\text{Max } J_1 = P_{\text{E}}\,[Q_1, F, m_1, m_2, m_4, \chi] = M^{\text{E}}_A/(M^{\text{E}}_A + M^{\text{E}}_B) \tag{11a}$$

$$\text{Max } J_2 = \text{Prod}\,[Q_1, F, m_1, m_2, m_4, \chi] = F \cdot C^{\text{F}}_{\text{T}}/V_{\text{solid}} \tag{11b}$$

$$\text{Subject to } P_{\text{R}} = M^{\text{R}}_B/(M^{\text{R}}_A + M^{\text{R}}_B) \geq 90\% \tag{11c}$$

$$\Delta P_{\text{unit}} \leq 70 \text{ bar} \tag{11d}$$

$$V_{\text{solid}} = 120 \text{ ml}, \Omega = 1 \text{ cm}^2 \text{ and fixed values of } N_{\text{col}}, C^{\text{F}}_{\text{T}}\ (x_A = x_B = 0.5) \text{ and } d_{\text{P}} \tag{11e}$$

where J_1 and J_2 are the two objective functions to be maximized, i.e. extract purity and productivity, respectively, while the optimization variables are the flow-rate in section 1, Q_1, the feed flow-rate, F, the flow-rate ratios, m_1, m_2 and m_4, and the unit configuration represented by the parameter, χ. It is worth noting that by fixing Q_1, F, m_1, m_2 and m_4, the five operating variables Q_1, Q_2, Q_3, Q_4 and t_{s} are unequivocally determined through Eq. (1) ($j = 1, \ldots, 4$) and the mass balance relationship $F = Q_3 - Q_2$. The total solid volume V_{solid} and the column cross-section Ω are fixed at 120 ml and 1 cm^2,

respectively. Actually, the cross-section value allows for the unit scale-up. Total number of columns N_{col}, feed concentration C_T^F (with equimolar composition of the two enantiomers) and particle diameter d_p are fixed in each optimization run, although various values have been considered to illustrate the unit behavior. Optimizations were carried out using the genetic algorithm, described in detail elsewhere [14,17].

5. Results and discussion

5.1. Role of the size of the packing material

As mentioned above, the particle diameter has a conflicting effect on the two objective functions under examination through the column efficiency (HETP) and the column pressure drop, as shown by Eqs. (2) and (3). In the following, we analyze the effect of this important parameter on the performance of the SMB and Varicol processes, while keeping the total number of columns N_{col} and the feed concentration C_T^F fixed at 5 and 8 g/l, respectively. For a five-column four-section set-up, there are four different column configurations, referred to in this paper by four values of the variable χ: A (2/1/1/1), B (1/2/1/1), C (1/1/2/1) and D (1/1/1/2), where (2/1/1/1) means two columns in section 1 and one each in sections 2, 3 and 4, etc.

The optimization results for the SMB unit are shown in Fig. 4 and Table 2 for three particle diameters: 40, 30 and 20 μm. In Fig. 4a one can see that, as expected, for each particle diameter a different Pareto curve is obtained, that is for increasing productivity values, the maximum possible purity of the extract decreases. Such Pareto curves are the typical solutions of multiobjective optimization prob-

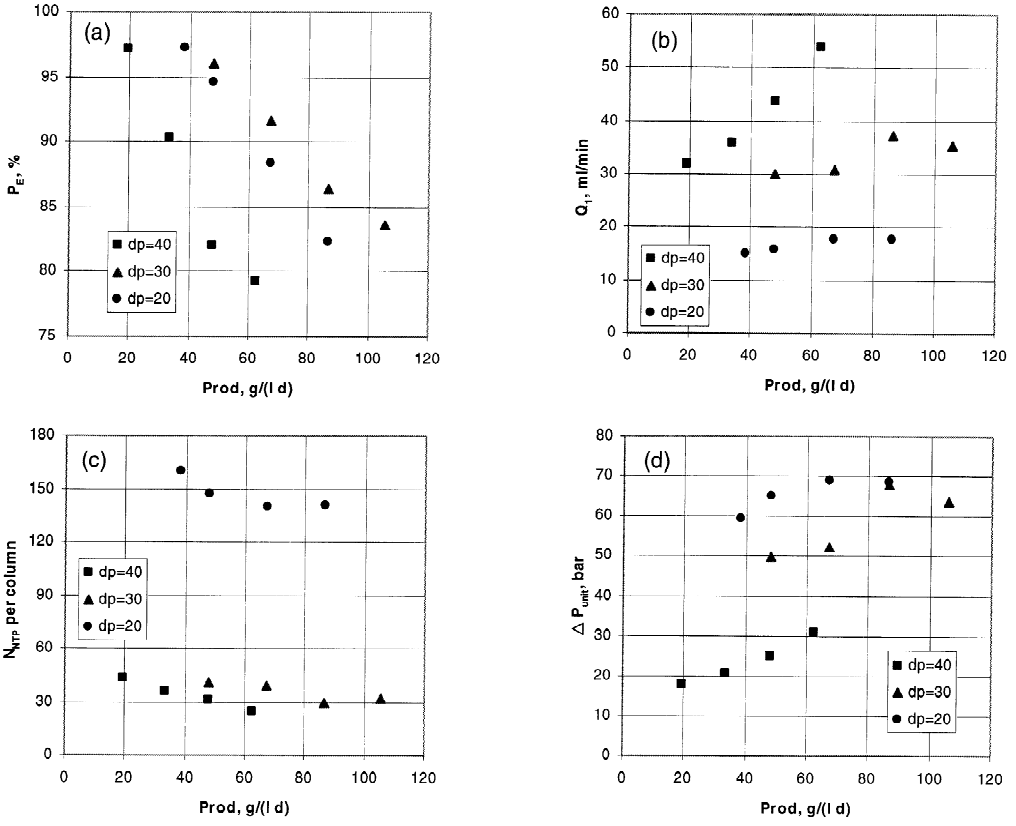

Fig. 4. Pareto solution of the optimization problem (Eq. (11)) with a SMB unit for various particle sizes.

Table 2
Optimization results for SMB and Varicol processes for three particle size d_p ($N_{col}=5$, $C_T^F=8$ g/l)

d_p (μm)	Process	Prod. (g/l day)	Q_1 (ml/min)	m_1	m_2	F (ml/min)	m_4	χ[a]	N_{NTP} per column	ΔP_{unit} (bar)	P_R (%)	P_E (%)
40	SMB	19.2	32.000	5.234	0.933	0.20	0.519	B	43	17.73	90.14	97.11
		33.6	35.940	4.803	0.855	0.35	0.691	B	36	20.66	90.00	90.32
		48.0	43.767	4.766	0.894	0.50	0.306	C	31	24.91	90.02	81.97
		62.4	53.757	4.632	0.889	0.65	0.262	C	25	30.89	90.00	79.33
	Varicol	33.6	37.070	5.224	0.876	0.35	0.278	C–B–B	39	20.11	90.00	93.28
		48.0	41.660	5.562	0.804	0.50	0.494	C–B–B	36	22.04	90.01	87.50
		62.4	55.580	5.179	0.842	0.65	0.180	C–C–B	27	29.92	90.02	84.01
30	SMB	48.0	30.000	1.700	0.900	0.50	0.720	B	41	49.78	90.27	96.00
		67.2	30.747	1.567	0.843	0.70	0.738	B	39	52.14	90.00	91.68
		86.4	37.174	1.350	0.883	0.90	0.706	C	30	67.83	90.01	86.43
		105.6	35.415	1.350	0.824	1.10	0.681	C	32	63.68	90.04	83.61
	Varicol	67.2	35.761	1.538	0.895	0.70	0.663	C–B–B	33	61.81	90.00	94.22
		86.4	38.378	1.500	0.852	0.90	0.612	C–B–B	31	66.07	90.28	90.41
		105.6	39.206	1.542	0.824	1.10	0.566	C–C–B	31	66.16	90.00	87.16
20	SMB	38.4	14.937	1.384	0.840	0.40	0.662	B	160	59.50	90.01	97.24
		48.0	15.821	1.275	0.805	0.50	0.756	B	147	65.04	90.02	94.61
		67.2	17.747	1.398	0.733	0.70	0.702	B	140	68.85	90.05	88.37
		67.2[b]	17.111	1.245	0.743	0.70	0.604	C	139	69.61	90.03	85.76
		86.4	17.706	1.332	0.662	0.90	0.687	B	141	68.71	90.03	82.31
		86.4[b]	17.250	1.258	0.670	0.90	0.626	C	140	69.01	90.04	80.24
	Varicol	The optimal Varicol coincides with SMB										

[a] B and C represent column configurations 1/2/1/1 and 1/1/2/1 where $N_{col}=5$, respectively.
[b] Results were obtained by fixing χ=C.

lems where we cannot decide between two optimal operating points, one of which leads to a better value of the first objective function and the other to a better value of the second. Meanwhile, the constraints on raffinate purity P_R and overall pressure drop ΔP_{unit} (Table 2 and Fig. 4d) are satisfied. In particular, the value of P_R is always equal to its lower bound (90%), as a consequence of the request of maximizing P_E and productivity, while ΔP_{unit} takes quite different values depending upon the particle diameter.

In Fig. 4a, we see that the particle diameter $d_p=40$ μm leads to the poorest performances. In this case, the SMB operates at the highest flow rates (see Q_1 in Fig. 4b) in order to increase productivity, but the low column efficiency (Fig. 4c) strongly limits the unit performance. It is worth noting that the latter and not the pressure drop limits the separation performance, as is shown in Fig. 4d where it is seen that pressure drop remains well below the upper limit of 70 bar. For the particle diameter $d_p=30$ μm, the column flow-rate Q_1 decreases while ΔP_{unit} increases as expected. For the same productivity value, say for example Prod=48 g/(l day), the N_{NTP} value increases from 31 for 40 μm to 41 for 30 μm. At these low column efficiency values, the advantage of this increase in N_{NTP} outweighs the disadvantage of the decrease in the flow-rates, thus leading to improved separation performances. Accordingly, for the same productivity value mentioned above, the SMB with 30-μm diameter particles leads to higher extract purity than that with 40-μm diameter particles, i.e. 96 versus 82%. For increasing productivity, Q_1 and ΔP_{unit} also increase while N_{NTP} decreases, until the pressure drop hits the upper bound of 70 bar at Prod=86.4 g/(l day). A further increase in productivity does not result in increasing flow-rate and pressure drop, which then becomes the parameter limiting the unit performance. At $d_p=20$ μm, the SMB unit operates at the lowest flow-rates in order to keep the pressure drop within the given upper bound, while the highest N_{NTP} values (above 140

under the conditions investigated) and then column efficiencies are achieved. In this case, the separation performance is limited by the pressure drop constraint rather than by the column efficiency. The result is that the unit performances become inferior to those obtained with 30-μm particle diameter, and the difference becomes more significant at high productivity, where the influence of pressure drop limitations is more important.

A physical interpretation of the optimization results reported above can be obtained in the frame of the triangle theory. For this, the operating conditions corresponding to the points on the Pareto sets in Fig. 4 are shown in Fig. 5 in terms of the flow-rate ratio parameters in the unit, i.e. m_1, m_2, m_3 and m_4. It is seen that for each particle size, m_1 is larger than its lower bound (given by $H_A = 1.25$) while m_4 is smaller than its upper bound (given by the relationship reported previously [21]), which guarantees proper regeneration of the solid and the mobile phases in sections 1 and 4, respectively. For the largest particle size, i.e. $d_p = 40$ μm, significantly higher m_1 and lower m_4 values have to be used to compensate for the low column efficiency, and this results in much higher eluent consumption. In Fig. 5 it is also seen that m_2 and m_3 decrease as productivity increases, which is due to the fact that since along the Pareto this implies that the extract purity decreases, the operating conditions in the m_2–m_3 parameter plane move towards the pure raffinate region, i.e. downwards to the left. This trend exhibits however a discontinuity in the value of m_2 and m_3 which, as it can be seen from the data in Table 2, corresponds to the configuration change from B to C. This happens because, as it is again apparent in Table 2, the increase in productivity has caused a decrease in the extract purity and therefore made the constraint on raffinate purity (90%) the controlling

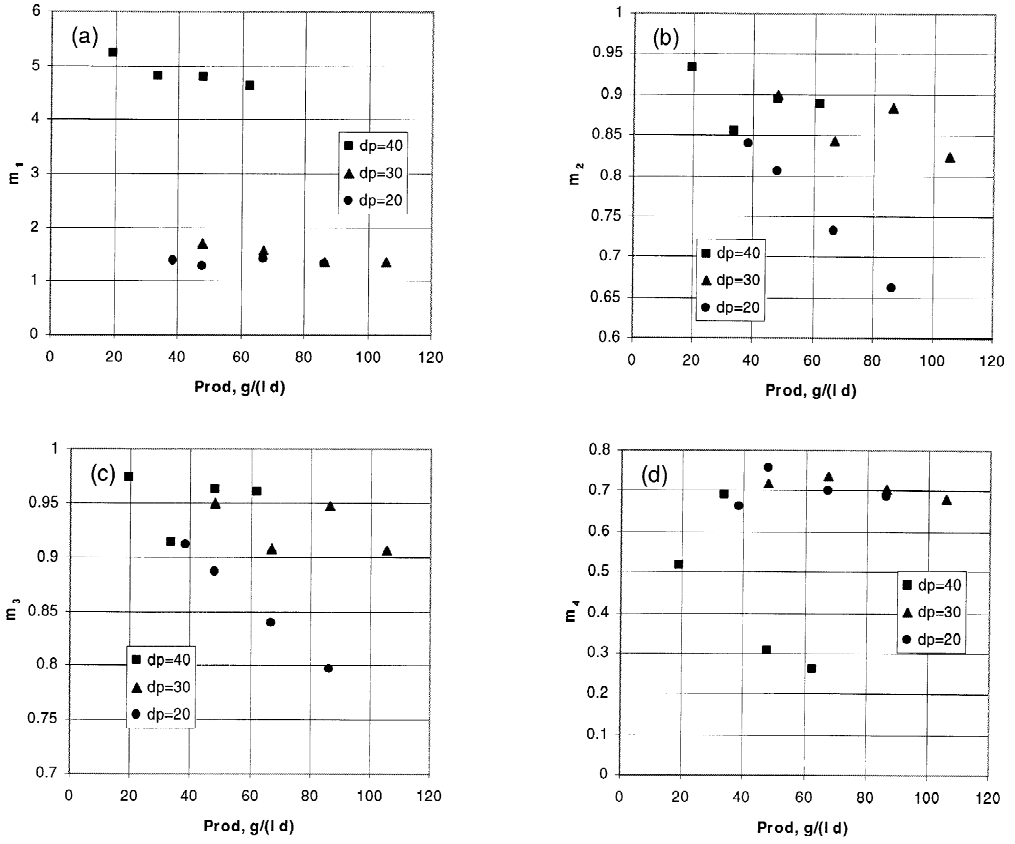

Fig. 5. Values of the flow-rate ratio parameters m_1 to m_4 corresponding to the points on the Pareto sets in Fig. 4.

one, thus requiring higher efficiency in section 3 with respect to that in section 2. This is obtained by moving one column from section 2 to section 3, i.e. changing from configuration $\chi = B$ to $\chi = C$. It is worth noting that at the smallest particle size, i.e. $d_p = 20$ μm, where the system is controlled by the pressure drop constraint, the column configuration change (from B to C) is not required. It is in fact the pressure drop limitation that prevents the appearance of configuration C, which implies a larger pressure drop in the unit than configuration B for the same productivity, since the flow-rates are larger in section 3 than in section 2. This has been confirmed by repeating the optimization for the productivity values of 67.2 and 86.4 g/(l day), while enforcing the configuration C. The results obtained are reported in Table 2 in the rows labeled with an asterisk. Compared to the operation with configuration B, it is seen that in this case the unit operates with lower Q_1 to compensate for the larger pressure drop in section 3, which eventually leads to lower extract purities.

The three-subinterval Varicol has also been investigated and found to be superior to the corresponding SMB for both particle diameters 30 and 40 μm, as shown in Fig. 6 and Table 2. It can be seen that for the same productivity, Varicol can reach higher P_E. The optimal column configuration changes from C–B–B to C–C–B with increasing productivity or decreasing P_E. Thus, similarly to SMB, Varicol also tends to transfer the extra column from section 2 to section 3, in order to improve the separation performance in terms of raffinate purity, at the expense of extract purity. However, the higher flexibility of Varicol allows a finer distribution of the columns in the two sections, which leads to better performances than SMB.

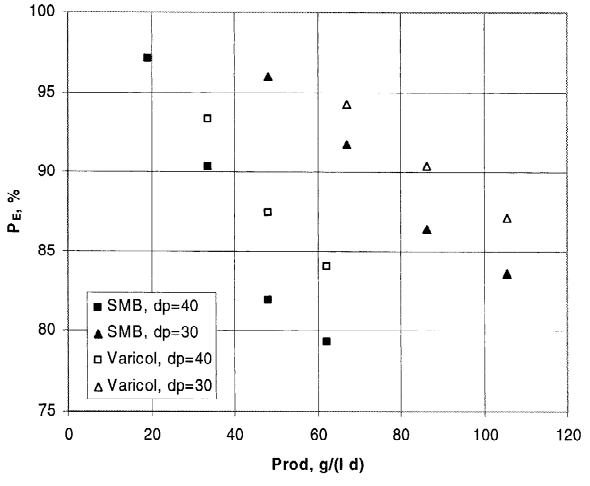

Fig. 6. Comparison of Pareto sets for SMB and Varicol for two packing sizes.

In the case of the smallest particle diameter, i.e. $d_p = 20$ μm, no Varicol configuration could be found that would be superior to the SMB configuration. So, for all productivity values the optimization algorithm converged to a SMB unit as the most convenient one. Indeed in Fig. 6, we observe that the performance difference between the optimized units decreases as d_p decreases, and we see now that it vanishes at $d_p = 20$ μm. The fact that at this particle size, the column efficiency is larger makes it difficult in general for Varicol to improve over SMB, and in addition the increase in pressure drop probably prevents using configuration C, which, as shown in Table 2, is how Varicol can improve over SMB in this particular case.

In conclusion, the optimization study conducted for the particular system under examination indicated that a SMB packed with 30-μm diameter particles achieves higher extract purity for a given productivity with the same raffinate purity and unit pressure drop than a SMB packed with 20- or 40-μm diameter particles. These are in fact prevented by unit pressure drop and column efficiency, respectively, to achieve further improvement. A three-subinterval Varicol is superior to the corresponding SMB when the system is not operated at too low particle diameters.

5.2. Role of the total number of columns

An important aspect in comparing SMB and Varicol processes is the effect of the total number of columns, N_{col}. It is in fact expected that as N_{col} increases, the discretization of the movement of the solid in the SMB improves and therefore the higher tunability of Varicol in this respect becomes less effective. The optimization results for SMB and Varicol are compared in Fig. 7 and Table 3 for a given productivity 67.2 g/(l day), a particle size of $d_p = 30$ μm, and for various values of N_{col}. Since the total solid volume V_{solid} and column cross-section Ω

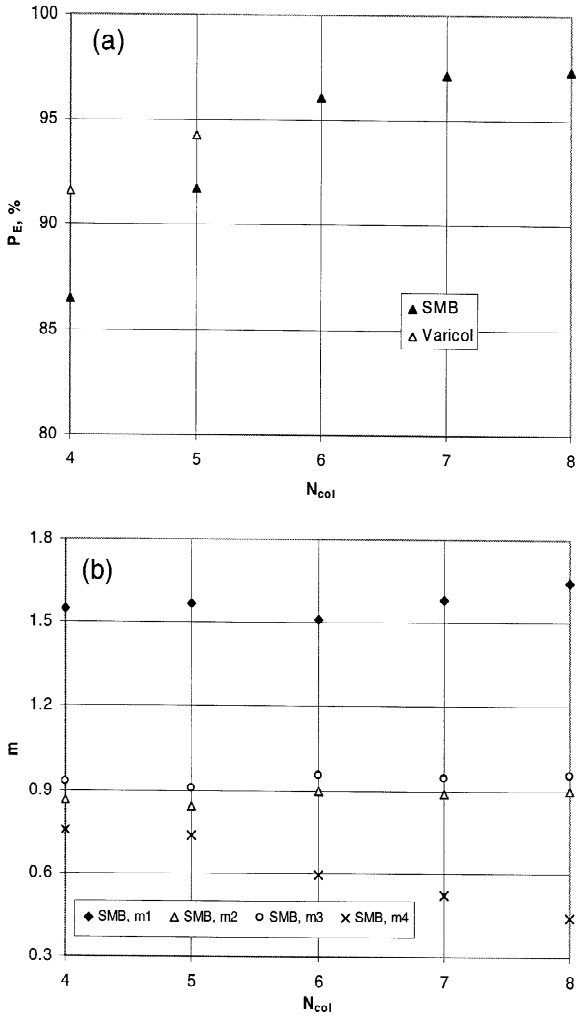

Fig. 7. Optimization of SMB and Varicol for various values of the total number of columns N_{col} and fixed productivity. (a) Purity of the extract; (b) Flow-rate ratio parameters m_1 to m_4.

are kept constant, changes in N_{col} imply changes in column length, L_{col}. It is seen that P_E increases with increasing column number, particularly at the lower values of N_{col}. P_E increases in fact by almost 10% from 86.5% for $N_{col}=4$ to 96.0% for $N_{col}=6$. A further increase in total number of columns has little influence on P_E. In addition, from a practical point of view, it is worth noting that the short switching time values caused by the short column lengths may lead to difficulties in the operation of the recycle pump. With respect to column configuration χ, the results in Table 3 indicate that all the additional columns tend to distribute equally between sections 2 and 3. This is because, once the lower bound on m_1 and the upper bound on m_4 are satisfied, sections 2 and 3 are the most important in determining P_E and P_R. The m_j values shown in Fig. 7b indicate that indeed in the cases under examination, both such constraints are satisfied.

In Fig. 7a, the performances of a three-subinterval Varicol for increasing values of the total number of columns is shown. It is seen that Varicol outperforms SMB only for $N_{col}=4$, and to a lower extent for $N_{col}=5$. When $N_{col}>5$, no Varicol configuration was found which improved P_E over the corresponding SMB value. Thus, as expected, for increasing total number of columns, the Varicol configuration is not worthwhile anymore. It is worth noting that in the case of $N_{col}=4$, the following five possible configurations have been considered for Varicol: 0/1/2/1, 0/2/1/1, 1/2/1/0, 1/1/2/0 and 1/1/1/1. The first four of such configurations have only three sections, which actually were not considered in the cases where $N_{col}>4$. As seen in Table 3, the configuration 0/1/2/1–0/2/1/1–1/1/1/1 was found to be optimal for the three-subinterval Varicol, which increases P_E by about 5% over the corresponding SMB with 1/1/1/1 configuration. It is interesting to note that in the first two subintervals there is no column in section 1; the fourth column moves in fact from section 3 in the first subinterval to section 2 in the second and eventually to section 1 in the last subinterval. This corresponds to the time-averaged configuration 0.33/1.33/1.33/1, which compared to the configuration 1/1/1/1 of the SMB, indicates that in this particular case Varicol improves the performance of the separation by reducing the length of section 1 and increasing that of sections 2 and 3.

5.3. Role of the total feed concentration

Apparently, the simplest way to increase productivity of a SMB or Varicol unit is to increase the total feed concentration, at least when this is allowed by solubility constraints. However, in most cases this makes the adsorption isotherms more nonlinear, thus making the separation more difficult. This is reflected in the narrowing of the complete separation region, shown in Fig. 3. In the following, we analyze

Table 3
Optimization results for SMB and Varicol processes for various values of the total number of columns N_{col} (d_p=30 μm, Prod=67.2 g/(l day), C_T^F=8 g/l)

Process	N_{col}	L_{col} (cm)	Q_1 (ml/min)	m_1	m_2	F (ml/min)	m_4	χ	N_{NTP} per column	ΔP_{unit} (bar)	P_R (%)	P_E (%)
SMB	4	30	30.328	1.550	0.867	0.70	0.754	1/1/1/1	48	52.79	90.02	86.49
	5	24	30.747	1.567	0.843	0.70	0.738	1/2/1/1	39	52.14	90.00	91.68
	6	20	35.126	1.512	0.900	0.70	0.594	1/2/2/1	28	60.47	90.07	96.04
	7	17.14	34.735	1.584	0.888	0.70	0.525	1/3/2/1	25	57.86	90.02	97.13
	8	15	36.595	1.643	0.900	0.70	0.444	1/3/3/1	21	59.86	90.06	97.29
Varicol	4	30	29.502	1.747	0.837	0.70	0.680	0/1/2/1–0/2/1/1 –1/1/1/1	55	48.40	90.01	91.55
	5	24	35.761	1.538	0.895	0.70	0.663	C-B-B	33	61.81	90.00	94.22

the effect of the total feed concentration on the optimal performances of SMB and Varicol by solving the optimization problem Eq. (11), with fixed N_{col}=5 and d_p=30 μm, for four different values of the total feed concentration, C_T^F. The Pareto curves obtained are compared in Fig. 8 and Table 4. In Fig. 8a it is seen that the SMB Pareto improves, by moving to higher productivities and extract purities, as the total feed concentration C_T^F increases from 6 to 24 g/l, although the extent of the improvement reduces significantly at the larger values of the total feed concentration, i.e. in the region between 14 and 24 g/l. This result, which was also reported by Biressi et al. [11], indicates that in the case under examination the SMB should operate at its maximum allowable feed concentration in order to obtain the highest productivities for given extract purities. However, from equilibrium theory, we know that the robustness of the operating conditions plays a significant role in cases where the complete separation region is so small as in Fig. 3 for C_T^F=24 g/l, since the system may become very sensitive to external disturbances. Therefore the optimal feed concentration must be determined by taking all these factors into account in practical applications.

In Fig. 8b and Table 4, it is seen that for the same feed concentrations, Varicol achieves higher productivities and extract purities than the corresponding SMB process. The extent of such improvement reduces with increasing P_E or decreasing productivity. This behavior is typical for units of this type [14]: in the case where only one very high purity product stream is required (asymmetric separations), the difference between Varicol and SMB reduces. For

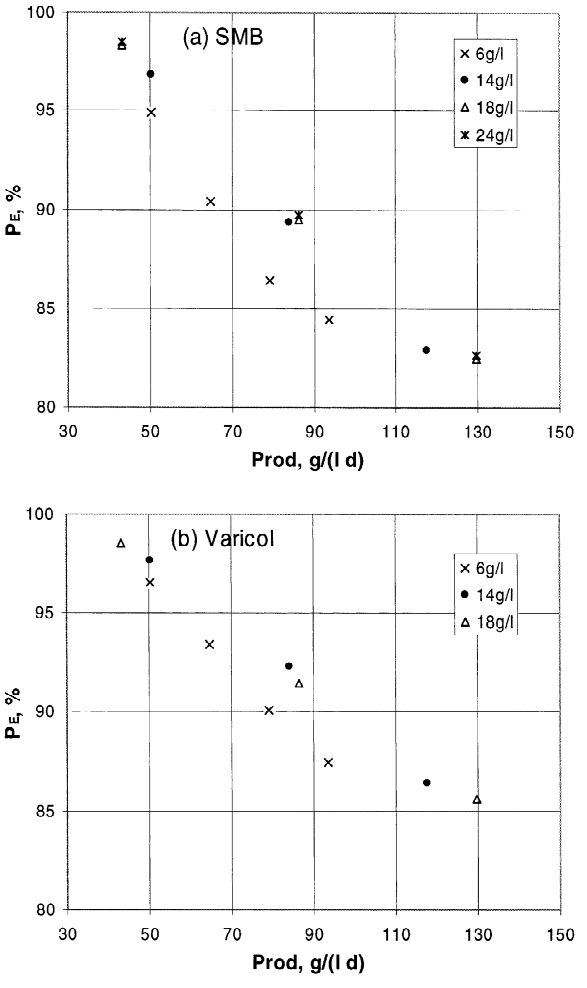

Fig. 8. Optimization Pareto sets for (a) SMB and (b) Varicol for various values of the total feed concentration.

Table 4
Optimization results for SMB and Varicol processes for various values of the total feed concentration C_T^F ($d_p = 30$ μm, $N_{col} = 5$)

C_T^F (g/l)	Process	Prod (g/l day)	Q_1 (ml/min)	m_1	m_2	F (ml/min)	m_4	χ	N_{NTP} per column	ΔP_{unit} (bar)	P_R (%)	P_E (%)
6	SMB	50.4	29.474	1.583	0.890	0.70	0.751	B	40	50.48	90.00	94.89
		64.8	27.583	1.484	0.826	0.90	0.734	B	42	47.71	90.00	90.38
		79.2	34.210	1.394	0.877	1.10	0.674	C	33	61.61	90.06	86.39
		93.6	36.867	1.386	0.854	1.30	0.628	C	31	65.98	90.00	84.44
	Varicol	50.4	31.548	1.475	0.929	0.70	0.688	C–B–B	36	56.13	90.00	96.50
		64.8	32.017	1.524	0.876	0.90	0.687	C–B–B	36	55.61	90.11	93.39
		79.2	33.972	1.670	0.831	1.10	0.692	C–B–B	36	56.34	90.01	90.04
		93.6	36.125	1.584	0.809	1.30	0.692	C–B–B	33	60.97	90.00	87.44
14	SMB	50.4	26.374	1.452	0.893	0.30	0.727	B	43	46.57	90.00	96.85
		84.0	31.704	1.530	0.805	0.50	0.698	B	38	53.46	90.01	89.34
		117.6	31.668	1.320	0.780	0.70	0.650	C	36	56.33	90.06	82.84
	Varicol	50.4	28.814	1.416	0.926	0.30	0.682	C–B–B	39	51.75	90.02	97.62
		84.0	33.884	1.597	0.840	0.50	0.689	C–B–B	36	56.84	90.01	92.30
		117.6	34.583	1.600	0.756	0.70	0.650	C–B–B	36	56.64	90.07	86.37
18	SMB	43.2	26.074	1.441	0.925	0.20	0.750	B	43	46.62	90.06	98.32
		86.4	30.198	1.445	0.797	0.40	0.698	B	39	51.95	90.00	89.48
		129.6	33.740	1.390	0.774	0.60	0.598	C	35	58.35	90.03	82.42
	Varicol	43.2	23.692	1.400	0.924	0.20	0.720	C–B–B	47	42.81	90.02	98.48
		86.4	28.125	1.411	0.804	0.40	0.694	C–B–B	41	49.10	90.03	91.43
		129.6	35.679	1.489	0.764	0.60	0.635	C–C–B	34	60.09	90.05	85.60
24	SMB	43.2	24.004	1.384	0.918	0.15	0.767	B	46	43.58	90.00	98.48
		86.4	28.226	1.399	0.788	0.30	0.694	B	41	49.02	90.02	89.69
		129.6	32.982	1.371	0.772	0.45	0.621	C	35	57.32	90.03	82.61

both SMB and Varicol, as shown in Table 4, m_2 as well as m_3 decrease with increasing productivity, due to the corresponding decrease in P_E. This behavior, as well as the discontinuity in the m_2 values due to the change in the unit configurations, has already been discussed earlier in the context of Fig. 5.

6. Conclusions

In this work, we investigated the SMB and Varicol processes, using a multiple objective optimization technique based on a genetic algorithm. This allows us to maximize simultaneously two objective functions, such as for example the purity of the extract and the productivity, under given constraints on the purity of raffinate and on the pressure drop in the entire unit. The equilibrium stage model, which accounts for real column efficiency, has been used to simulate the SMB and Varicol process. Using this optimization tool, it is possible to optimize and compare the performances of SMB and Varicol in a wide range of parameter values (for example accounting also for the column configuration), so as to clearly assess their relative potential under equally optimized conditions. The effect of three variables of significant impact on the economy of the separation has been examined: the particle size of the packing material, the total number of columns and the total feed concentration. In all cases clear quantitative results have been obtained for the particular separation taken as model system. Although it is difficult to generalize these results, it can be concluded that for both SMB and Varicol, there exists in general an optimum packing size. The performances of these units increase asymptotically with the total number of columns, the maximum convenient value probably being around 6–8 depending on the specific case. For the total feed concentration, considerations about solubility limit and process robustness most likely

become the limiting factors. Regarding the comparison between SMB and Varicol, the second provides consistently better performances, although the improvement becomes negligible at total numbers of columns larger than 5–7. It remains to be said that for any given separation, the optimal conditions have to be calculated ad hoc in order to make the proper choice of the most convenient unit.

7. Nomenclature

a, b, c	parameters of the HETP equation
$C_i^{(k)}$	liquid phase concentration of component i in stage k, g/l
$\overline{C_i^{(k)}}$	solid-phase concentration of component i in stage k, g/l
C_T^F	total feed concentration, g/l
d_p	particle diameter, μm
D	eluent flow-rate, ml/min
E_N	error function denoting mass balance during the Nth switching period
E	flow-rate of extract stream, ml/min
F	feed flow-rate, ml/min
H_i	Henry constant of component i
HETP	Height equivalent to a theoretical plate, cm
J	objective function
L_{col}	length of each column, cm
m	flow-rate ratio parameter
M_i	mass of component i collected or introduced during one switching period, g
n	number of columns
N_{col}	total number of columns
N_{NTP}	number of theoretical plates
ΔP	column pressure drop, bar
ΔP_{unit}	unit pressure drop, bar
Prod	productivity, g/(l day)
P_E	purity of extract stream, %
P_R	purity of raffinate stream, %
Q_j	fluid flow-rate in section j, ml/min
R	flow-rate of raffinate stream, ml/min
t	time, min
t_0	retention time of an inert component, min
t_s	switching time, min
u	velocity, cm/s
V_{col}	column volume, ml
V_{solid}	total solid volume, ml
x	mol fraction

Greek letters

χ	column configuration
ε	total porosity
ε_b	bed porosity
ε_p	particle porosity
μ	fluid viscosity
φ	constant of pressure drop correlation
Ω	column cross-section, cm^2

Subscripts and superscripts

A	strong component of the feed
B	weak component of the feed
i	component i
j	section j
k	kth mixing cell
N	Nth switching period
M	Mth subinterval in Varicol
T	total

Acknowledgements

Partial financial support from the KTI project 4020.2 is kindly acknowledged.

References

[1] H.-K. Rhee, R. Aris, N. Amundson, in: First-order Partial Differential Equations, Vol. II, Prentice-Hall, Englewood Cliffs, NJ, 1989.
[2] G. Storti, M. Mazzotti, M. Morbidelli, S. Carra, AIChE J. 39 (1993) 471.
[3] M. Mazzotti, G. Storti, M. Morbidelli, AIChE J. 40 (1994) 1825.
[4] M. Mazzotti, G. Storti, M. Morbidelli, AIChE J. 42 (1996) 2784.
[5] M. Mazzotti, G. Storti, M. Morbidelli, AIChE J. 43 (1997) 64.
[6] G. Storti, R. Baciocchi, M. Mazzotti, M. Morbidelli, Ind. Eng. Chem. Res. 34 (1995) 288.
[7] F. Charton, R.M. Nicoud, J. Chromatogr. A 702 (1995) 97.
[8] G. Dunnebier, K.U. Klatt, Comput. Chem. Eng. 23 (1999) S195.

[9] S. Karlsson, F. Pettersson, T. Westerlund, Comput. Chem. Eng. 23 (1999) S487.
[10] C. Migliorini, A. Gentilini, M. Mazzotti, M. Morbidelli, Ind. Eng. Chem. Res. 38 (1999) 2400.
[11] G. Biressi, O. Ludemann-Hombourger, M. Mazzotti, R.M. Nicoud, M. Morbidelli, J. Chromatogr. A 876 (2000) 3.
[12] K.U. Klatt, F. Hanisch, G. Dunnebier, J. Process Contr. 12 (2002) 203.
[13] A. Jupke, A. Epping, H. Schmidt-Traub, J. Chromatogr. A 944 (2002) 93.
[14] Z.Y. Zhang, K. Hidajat, A.K. Ray, M. Morbidelli, AIChE J. (2002) in press.
[15] O. Ludemann-Hombourger, R.M. Nicoud, M. Bailly, Sep. Sci. Technol. 35 (2000) 1829.
[16] O. Ludemann-Hombourger, G. Pigorini, R.M. Nicoud, D.S. Ross, G. Terfloth, J. Chromatogr. A 947 (2002) 59.
[17] V. Bhaskar, S.K. Gupta, A.K. Ray, Rev. Chem. Eng. 16 (2000) 1.
[18] D.M. Ruthven, C.B. Ching, Chem. Eng. Sci. 44 (1989) 1011.
[19] A. Gentilini, C. Migliorini, M. Mazzotti, M. Morbidelli, J. Chromatogr. A 805 (1998) 37.
[20] G. Guiochon, S.G. Shirazi, A.M. Katti, Fundamentals of Preparative and Nonlinear Chromatography, Academic Press, Boston, MA, 1994.
[21] M. Mazzotti, G. Storti, M. Morbidelli, J. Chromatogr. A 769 (1997) 3.